The BAR domain of amphiphysin is required for cleavage furrow tip–tubule formation during cellularization in *Drosophila* embryos

Jing Su[a], Brenda Chow[a,b], Gabrielle L. Boulianne[a,b], and Andrew Wilde[a,c]
[a]Department of Molecular Genetics and [c]Department of Biochemistry, University of Toronto, Toronto, ON M5S 1A8, Canada; [b]Program in Developmental and Stem Cell Biology, The Hospital for Sick Children, Toronto, ON M5G 1X8, Canada

ABSTRACT **De novo formation of cells in the *Drosophila* embryo is achieved when each nucleus is surrounded by a furrow of plasma membrane. Remodeling of the plasma membrane during cleavage furrow ingression involves the exocytic and endocytic pathways, including endocytic tubules that form at cleavage furrow tips (CFT-tubules). The tubules are marked by amphiphysin but are otherwise poorly understood. Here we identify the septin family of GTPases as new tubule markers. Septins do not decorate CFT-tubules homogeneously: instead, novel septin complexes decorate different CFT-tubules or different domains of the same CFT-tubule. Using these new tubule markers, we determine that all CFT-tubule formation requires the BAR domain of amphiphysin. In contrast, dynamin activity is preferentially required for the formation of the subset of CFT-tubules containing the septin Peanut. The absence of tubules in amphiphysin-null embryos correlates with faster cleavage furrow ingression rates. In contrast, upon inhibition of dynamin, longer tubules formed, which correlated with slower cleavage furrow ingression rates. These data suggest that regulating the recycling of membrane within the embryo is important in supporting timely furrow ingression.**

Monitoring Editor
Anne Spang
University of Basel

Received: Dec 12, 2012
Revised: Feb 19, 2013
Accepted: Feb 21, 2013

INTRODUCTION

The reorganization and movement of membranes within a eukaryotic cell enables communication between organelles, cell migration, and cell division. Membrane reorganization through remodeling requires membrane deformation, which can occur in multiple ways. Membrane reorganization can be driven through proteins that stimulate localized membrane curvature. These curved membranes can be extruded further to form tubules or pinch off from the rest of the membrane to form a vesicle (Hurly *et al.*, 2010). On a larger scale, deformation of the membrane, in particular the plasma membrane, is driven through force applied over a wider region of the membrane by the cytoskeleton, for example, the actomyosin cytoskeleton during cell migration and cytokinesis (Ridley, 2011; Levayer and Lecuit, 2012). These mechanisms, either in isolation or when combined, can achieve a significant reorganization of cellular membranes.

Pseudocleavage furrow formation in the syncytial embryo of *Drosophila* is a dramatic example of plasma membrane reorganization that occurs during interphase and mitosis (Mazumdar and Mazumdar, 2002). Plasma membrane furrows ingress from the surface of the embryo to separate adjacent nuclei sharing a common cytoplasm. In the early stages of embryo development, between nuclear cycles 10 and 13, the pseudocleavage furrows ingress but do not meet. Instead they regress to the surface of the embryo during the later stages of mitosis. Such a mechanism allows nuclei to continue to share a common cytoplasm but prevents chromosome missegregation through multipolar spindle formation during mitosis. During the 14th nuclear cycle, cleavage furrows, which closely resemble pseudocleavage furrows, ingress and on this occasion

This article was published online ahead of print in MBoC in Press (http://www.molbiolcell.org/cgi/doi/10.1091/mbc.E12-12-0878) on February 27, 2013.
Address correspondence to: Andrew Wilde (andrew.wilde@utoronto.ca).
Abbreviation used: CFT, cleavage furrow tip.

they eventually meet and fuse to enclose each nucleus, leading to the production of ~6000 columnar epithelial cells, each with a unique cytosol. This de novo production of cells, called cellularization, shares many characteristics with cytokinesis; in particular, the cellular machinery that drives membrane ingression during cytokinesis also localizes to the ingressing cleavage furrow.

Cleavage furrow ingression depends on both the actomyosin and microtubule cytoskeletons. Microtubules are required only very early in the process to establish an actin cap above the newly forming nucleus during telophase of the previous cell cycle (Riggs *et al.*, 2007). Subsequently the actin cap expands and then drives furrow ingression. As furrows ingress, they are stabilized by anillin (Field *et al.*, 2005a), a protein that has the capacity to link the actomyosin and septin cytoskeletons to the plasma membrane (Liu *et al.*, 2012). Furrow ingression is not just a matter of applying force to the plasma membrane to move it: additional membrane must be added via the exocytic and recycling endosome pathways, mostly at the apical surface (Pelissier *et al.*, 2003). Furrow ingression also requires remodeling of the plasma membrane through endocytosis (Pelissier *et al.*, 2003; Sokac and Wieschaus, 2008a). Endocytosis occurs at two sites: at the apical surface (Pelissier *et al.*, 2003) and at the tip of the ingressing furrow (Sokac and Wieschaus, 2008a). Endocytosis at the cleavage furrow tip occurs through a poorly characterized mechanism that involves the formation of cleavage furrow tip tubules (CFT-tubules), which can be several microns long and eventually pinch off (Sokac and Wieschaus, 2008a).

CFT-tubule dynamics is regulated by the actin cytoskeleton (Sokac and Wieschaus, 2008a,b). In the absence of actin, CFT-tubules are more extensive (Sokac and Wieschaus, 2008a,b), suggesting that actin has a role in the pinching-off process. Indeed, actin has been demonstrated to have a role at different stages of endocytosis in different model systems, including yeast (Kaksonen *et al.*, 2003, 2005; Sun *et al.*, 2006), *Drosophila* (Kochubey *et al.*, 2006), and mammalian cells (Merrifield *et al.*, 2002; Yarar *et al.*, 2005). Further evidence that altered pinching-off dynamics may play a role in CFT-tubule organization was found when elongated CFT-tubules were observed upon dynamin inhibition (Sokac and Wieschaus, 2008b). Dynamin is a GTPase recruited to the neck of budding vesicles, where it has been implicated to function in the final pinching-off stage of vesicle formation (Schmid and Frolov, 2011).

What factors drive CFT-tubule formation is unclear. Proteins localizing to the tip of the ingressing furrow are likely players in CFT-tubule formation. There are two primary candidates, amphiphysin and septins, as each is capable of tubulating liposomes in vitro (Takei *et al.*, 1999; Tanaka-Takiguchi *et al.*, 2009). Amphiphysin is a BAR domain–containing protein that localizes to the furrow tip and CFT-tubules and was used as the marker to define CFT-tubules in previous studies (Sokac and Wieschaus, 2008a,b). The BAR domain of amphiphysin is capable of generating membrane curvature (Takei *et al.*, 1999). In addition, septins, a family of filamentous G-proteins (Saarikangas and Barral, 2011), localize to the tip of the ingressing pseudocleavage furrow (Neufeld and Rubin, 1994). Septins have an essential role in cytokinesis, but in addition they are increasingly associated with other cellular functions (reviewed in Saarikangas and Barral, 2011; Spiliotis and Gladfelther, 2011; Mostowy and Cossart, 2012). Septins can stimulate membrane tubulation in vitro on liposomes that contain phosphatidylinositol phosphates (Tanaka-Takiguchi *et al.*, 2009). Therefore multiple factors that can initiate, stabilize, or regulate membrane tubulation are positioned at the tips of ingressing cleavage furrows.

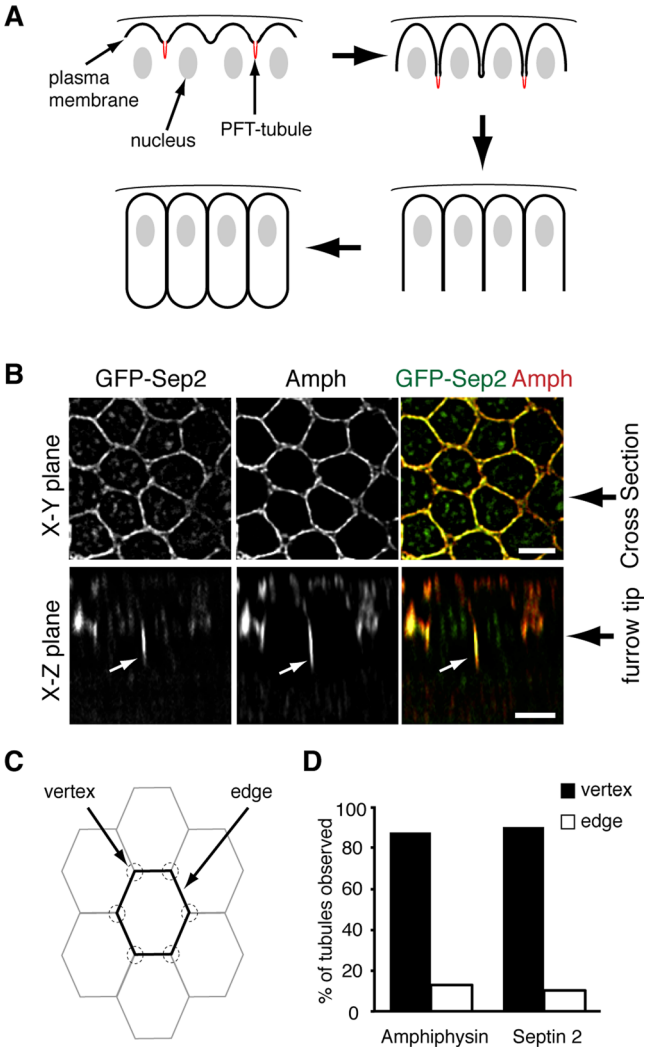

FIGURE 1: Septin 2 localizes to CFT-tubules that form at the vertices of intersecting cleavage furrows. (A) Cartoon outlining cleavage furrow ingression dynamics during cellularization in the syncytial *Drosophila* embryo. CFT-tubules are in red. (B) Confocal images of GFP-Sep2 and amphiphysin (Amph) localization in *Drosophila* embryos. Top, surface views; bottom, *z*-sections. White arrows indicate CFT-tubules. Bar, 5 µm. (C) Cartoon outlining the hexagonal membrane organization in *Drosophila* embryos. (D) Quantification of the localization of tubules positive for amphiphysin or Sep2-GFP relative to the vertex of intersecting cleavage furrows. The data are the combined number of tubules observed in at least 10 embryos for each condition.

One difficulty in studying the role of the CFT-tubules during furrow ingression is the lack of markers for them. Here we identify septins as new markers of CFT-tubules and examine the role of dynamin and amphiphysin in CFT-tubule regulation and how this correlates with cleavage furrow ingression dynamics. Our findings suggest that the regulation of membrane dynamics through endocytosis at the furrow tip may regulate membrane availability to drive efficient furrow ingression.

RESULTS

Septins localize to CFT-tubules

One site of endocytosis in the syncytial *Drosophila* embryo occurs at the tip of ingressing cleavage furrows (Figure 1A). Both endocytic

vesicles and elongated tubules are observed at the furrow tip, suggesting that this may be the site of a specialized form of endocytosis (Sokac and Wieschaus, 2008a). Previous studies that characterized CFT-tubules used amphiphysin as a marker to define them. However, to further understand the role of CFT-tubules in cellularization, it was necessary to identify further factors associated with the tubules. Using available antibodies and transgenic *Drosophila* lines expressing green fluorescent protein (GFP) fusion proteins, we searched for new CFT-tubule markers. Using this strategy, we identified septins, a family of filamentous GTPases, as novel CFT-tubule markers.

We previously showed that a GFP-tagged Sep2 transgene, when expressed in the early *Drosophila* embryo, localizes to the tips of pseudocleavage furrows during syncytial nuclear divisions in early *Drosophila* embryogenesis (Silverman-Gavrila *et al.*, 2008). Further analysis of Sep2-GFP during cellularization revealed that it localized not only to the ingressing cleavage furrow tip, but also to tubular extensions, CFT-tubules, emanating from the tip of some ingressing cleavage furrows (Figure 1B, white arrows). Of CFT-tubules decorated with Sep2-GFP, 93% also contained amphiphysin throughout the length of the CFT-tubule.

Intriguingly, CFT-tubules did not emanate from every furrow tip observed. We examined the position of CFT-tubules within the embryo to determine whether there was a defined distribution that may suggest function. There was no discernible pattern of CFT-tubules throughout the embryo, that is, CFT-tubules did not appear in a banded pattern or at greater concentrations at the anterior or the posterior of the embryo. However, 87% of amphiphysin-positive CFT-tubules and 90% of Sep2-GFP–positive CFT-tubules localized within 1 μm of the vertex of intersecting cleavage furrows (Figure 1, B and C), suggesting that CFT-tubules may regulate cleavage furrow organization.

Sep2 is part of a family of related proteins, the septins, that can form heterologous filamentous complexes (reviewed in Saarikangas and Barral, 2011; Mostowy and Cossart, 2012). In *Drosophila melanogaster* there are five septins—Sep1, Sep2, Peanut, Sep4, and Sep5—all of which are expressed in the early embryo (Graveley *et al.*, 2011). Sep2 has been isolated from *Drosophila* embryos in a complex with Sep1 and Peanut (Field *et al.*, 1996). Because septins in other species have been attributed differing functions (reviewed in Saarikangas and Barral, 2011; Spiliotis and Gladfelther, 2011; Mostowy and Cossart, 2012), we examined the localization of the other *Drosophila* septins during cellularization. To analyze other septin family members, we generated transgenic *Drosophila* lines that expressed different septin family members. Carboxy-terminal, septin-GFP fusions were expressed in the female germline (Rorth, 1998). Peanut-GFP was expressed in the syncytial embryo at levels below that of endogenous Peanut (Figure 2A). Owing to the lack of specific antibodies, we were not able to quantitatively assess the level of other septin-GFPs compared with endogenous proteins, but all other septin-GFPs were expressed at lower levels than Peanut-GFP (Figure 2B). These data suggest that the septin-GFPs were expressed below endogenous levels, allowing trace labeling of septin complexes and avoiding overexpression artifacts.

All septin-GFP fusion proteins localized, as expected, to the tips of ingressing cleavage furrows (Figure 3A). In addition, endogenous Peanut (Figure 4B) and all Septin-GFP fusions localized to CFT-tubules (Figure 3A). The CFT-tubules to which the septins localized were not randomly distributed: instead, ~90% of the CFT-tubules for each of the septins localized within 1 μm of the vertex of intersecting furrows (Figure 3B). Therefore septins are new markers of CFT-tubules.

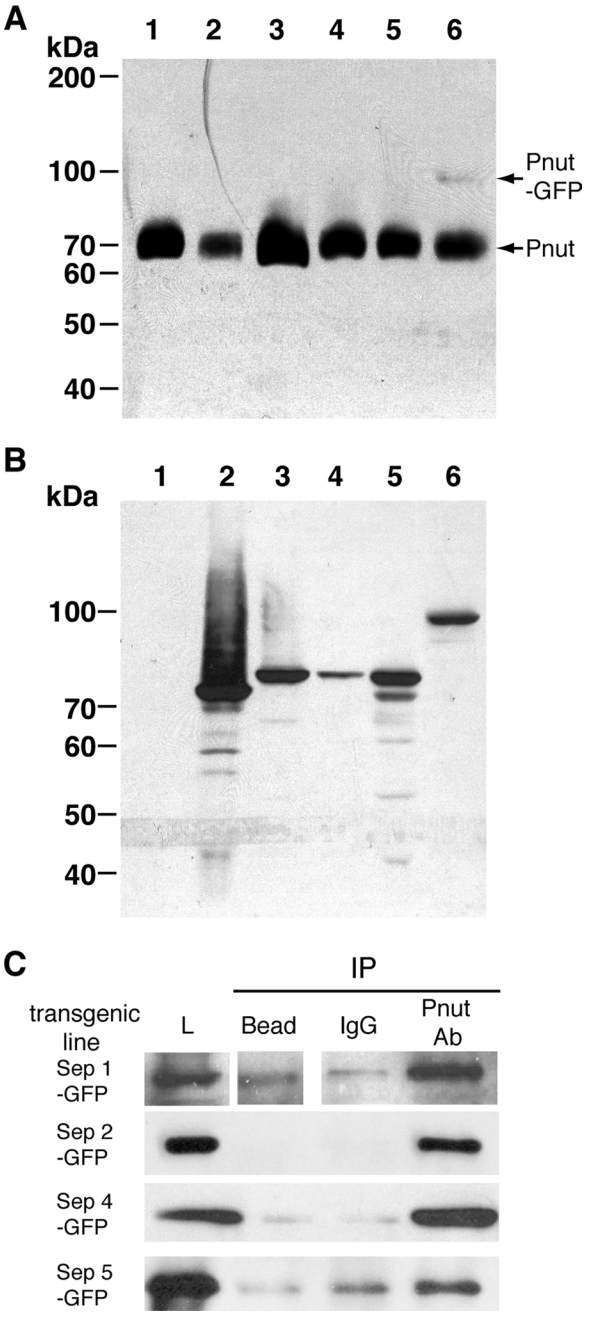

FIGURE 2: Expression levels of the different septin-GFPs. (A) A 1-mg extract of embryo from the different transgenic lines was loaded per lane and immunoblotted with an anti-Pnut mouse monoclonal antibody. 1, w1118; 2, Sep1-GFP; 3, Sep2-GFP; 4, Sep4-GFP; 5, Sep5-GFP; 6, Pnut-GFP. (B) A 1-mg extract of embryo from the different transgenic lines was loaded per lane and immunoblotted with an anti-GFP mouse monoclonal antibody. 1, w1118; 2, Sep1-GFP; 3, Sep2-GFP; 4, Sep4-GFP; 5, Sep5-GFP; 6, Peanut-GFP. (C) Pnut was immunoprecipitated (IP) from 10 mg of embryo lysates generated from the different septin-GFP transgenic lines. IPs were then analyzed by immunoblotting using an anti-GFP antibody to detect the septin-GFP fusion. L, embryo lysates.

A new complex of septins defines distinct CFT-tubule subdomains

During cell division, different septins localize to different cellular structures (Spiliotis *et al.*, 2005) and have been attributed different functions (Estey *et al.*, 2010). To determine whether septins associated

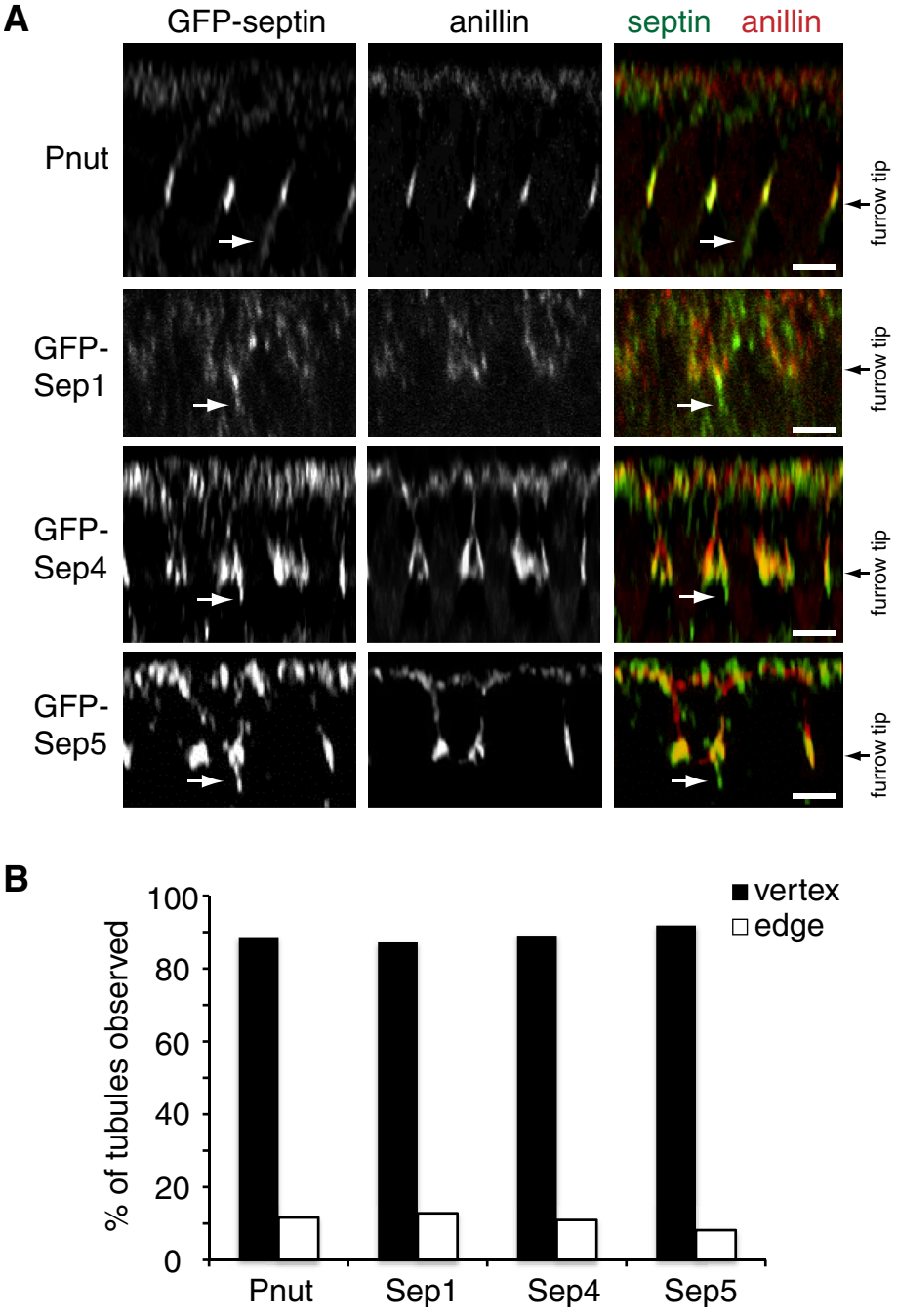

FIGURE 3: All septins localize to CFT-tubules at the vertices of intersecting cleavage furrows. (A) The *z*-sections of embryos expressing Pnut-GFP, Sep1-GFP, Sep4-GFP, or Sep5-GFP and immunostained with an anti-anillin antibody to mark the furrow tip. Bar, 5 μm. (B) Quantification of the localization of tubules positive for different septin-GFP fusion proteins relative to the vertex of intersecting cleavage furrows. The data are the combined number of tubules observed in at least 10 embryos for each condition.

with all CFT-tubules or subpopulations of CFTs, we compared the distribution of septin-positive CFT-tubules with amphiphysin-positive CFT-tubules within the same embryo. Of interest, not all CFT-tubule markers colocalized (Figure 4). In some cases entire tubules were labeled with some but not all septins (Figure 4, A–C). In other instances a single tubule possessed distinct domains labeled with different septin family members (Figure 4E), indicating that there are different CFT-tubule populations and distinct domains on CFT-tubules.

Sep2-GFP and Sep1-GFP demonstrated a high degree of colocalization with amphiphysin: 93% of CFT-tubules positive for Sep2-GFP (Figure 1A) and 95% of Sep1-GFP positive CFT-tubules (Figure 4A) also contained amphiphysin in all embryos examined. In contrast, Peanut and amphiphysin showed poor colocalization: only 11% of CFT-tubules were positive for both amphiphysin and Peanut, whereas 49% were positive for amphiphysin alone and 40% were positive for Peanut alone (Figure 4, B and C). Sep4-GFP and Sep5-GFP localization was reminiscent of the Peanut distribution within the embryo as opposed to Sep1-GFP or Sep2-GFP distribution within the embryo. Only 13% of Sep4-GFP–positive CFT-tubules and 10% of Sep5-GFP–positive CFT-tubules were also positive for amphiphysin. In contrast, 56% of Sep4-GFP– and 43% of Sep5-GFP–labeled CFT-tubules were devoid of amphiphysin. Furthermore, Sep4-GFP and Sep5-GFP always colocalized with Peanut on CFT-tubules. Further analysis of CFT-tubules positive for amphiphysin and Peanut revealed that amphiphysin did not colocalize with the Peanut throughout the length of the tubule. Instead, the tubule consisted of distinct domains containing either Peanut or amphiphysin (Figure 4E). Similarly, pairwise analysis of Sep4-GFP or Sep5-GFP and amphiphysin found that these septins also did not colocalize with amphiphysin on CFT-tubules positive for both markers. There was no set pattern of amphiphysin-positive domains in relation to Peanut-, Sep4-, Sep5-positive domains on CFT-tubules. For example, Peanut-positive domains could be localized close to the tip of the CFT-tubule or close to the cleavage furrow. These data suggest that distinct septin complexes can define different subpopulations of CFT-tubules and different subdomains within CFT-tubules.

Peanut, Sep1, and Sep2 have been isolated as a single 2:2:2 complex from *Drosophila* embryo extracts (Field *et al.*, 1996). However, the differential spatial organization of septin family members on CFT-tubules suggests that Sep1 and Sep2 may be able to form a complex independently of Peanut. Specifically, our localization studies suggested that Peanut, Sep4, and Sep5 may form a complex. To examine this further, we immunoprecipitated Peanut using an antibody that recognized Peanut (Neufeld and Rubin, 1994). We found that Peanut could be coimmunoprecipitated with any other septin from *Drosophila* embryo extracts (Figure 2C), suggesting that multiple complexes may coexist or assemble in embryo extracts. Similar results were described in mammalian systems (Estey *et al.*, 2010). These data suggest that although a distinct Peanut–Sep4–Sep5 complex and another Sep1–Sep2 complex may

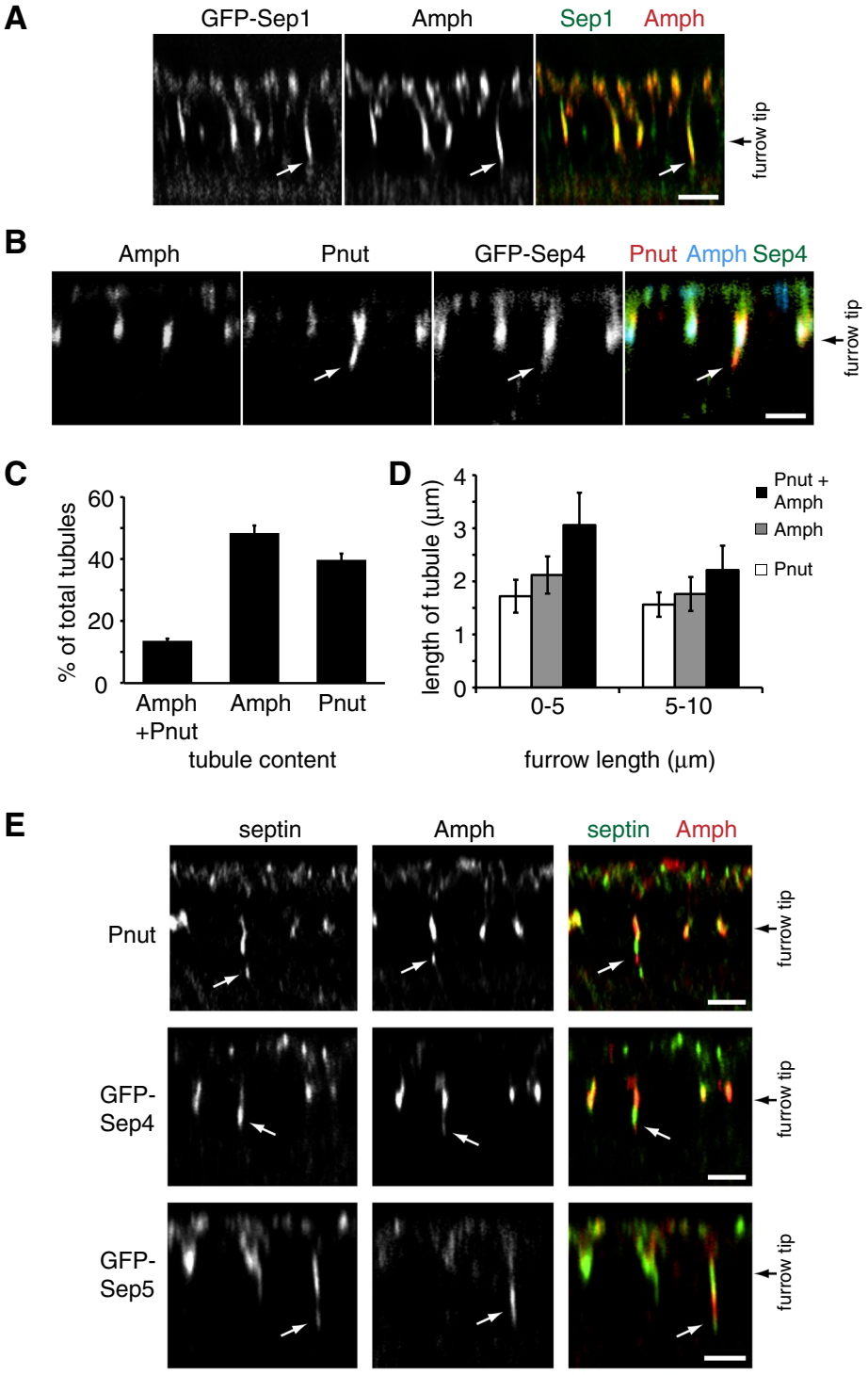

FIGURE 4: Different subpopulations of CFT-tubules are defined by different septin complexes. (A) A *z*-section of an embryo from a Sep1-GFP–expressing *Drosophila* line immunostained with an anti-amphiphysin (Amph) antibody. White arrows point to CFT-tubules. (B) A *z*-section of an embryo from a Sep4-GFP–expressing *Drosophila* line immunostained with an anti-amphiphysin (Amph) antibody and an anti-Pnut antibody. White arrows point to CFT-tubules. (C) Quantification of the number of CFT-tubules that stain uniquely with Pnut or amphiphysin (Amph) and CFT-tubules that possess both markers. Error bars, ±SD. $n = 11$ embryos. (D) Quantification of the length of different CFT-tubule populations at different stages of cleavage furrow ingression. Error bars, ±SD. $n = 11$ embryos. (E) Different septin-GFP–expressing embryos stained with an anti-amphiphysin (Amph) antibody that define CFT-tubules that have different septin and amphiphysin subdomains. White arrows point to CFT-tubules. Bar, 5 µm.

exist on CFT-tubules, other heterologous complexes made up of different septin combinations, including the previously isolated Peanut–Sep1–Sep2 complex (Field *et al.*, 1996), exist at the tips of ingressing cleavage furrows.

Amphiphysin CFT-tubules are dynamic and are detected at the early stages of furrow ingression (0–5 µm) but disappear at later stages (>5 µm; Sokac and Wieschaus, 2008a). We found that amphiphysin-containing CFT-tubules were longer than Peanut CFT-tubules, with the longest tubules being those that contained both Peanut and amphiphysin (Figure 4D). At early stages for furrow ingression (0–5 µm in depth), Peanut-only CFT-tubules were on average 1.7 µm (±0.3 µm; 33 tubules in five embryos) long, compared with uniquely amphiphysin-positive CFT-tubules and mixed CFT-tubules, which were 2.1 µm (±0.4 µm; 37 tubules from five embryos) and 3.1 µm (±0.6 µm; 36 tubules from five embryos) long, respectively (Figure 4D). When the cleavage furrow ingressed further to between 5 and 10 µm in depth, the CFT-tubules were shorter. Peanut CFT-tubules (1.6 ± 0.2 µm long; 49 tubules from eight embryos) were still shorter than amphiphysin-positive CFT-tubules (amphiphysin-only CFT-tubules, 1.8 ± 0.3 µm, 52 tubules from eight embryos; and mixed CFT-tubules, 2.2 ± 0 .5 µm, 44 tubules from eight embryos). These data suggest that the different CFT-tubule subpopulations may be differentially regulated in their formation, stability, or pinching-off rate.

Dynamin is required for Peanut- but not amphiphysin-positive CFT-tubule formation

Previous studies demonstrated a role for dynamin in regulating CFT-tubule organization (Sokac and Wieschaus, 2008a). Using the temperature-sensitive dynamin mutant *shibire*^{ts}, we also found that CFT-tubules were longer at the nonpermissive temperature (Figure 5A), as previously reported (Sokac and Wieschaus, 2008a). We next assessed the role of dynamin in regulating the different populations of CFT-tubules. In *shibire*^{ts} embryos, the total number of CFT-tubules per embryo remained the same at the nonpermissive and permissive temperatures. However, the relative proportion of the different CFT-tubules changed. At the nonpermissive temperature the number of uniquely Peanut-positive CFT-tubules decreased ($p < 0.0001$), whereas the number of amphiphysin-positive CFT-tubules

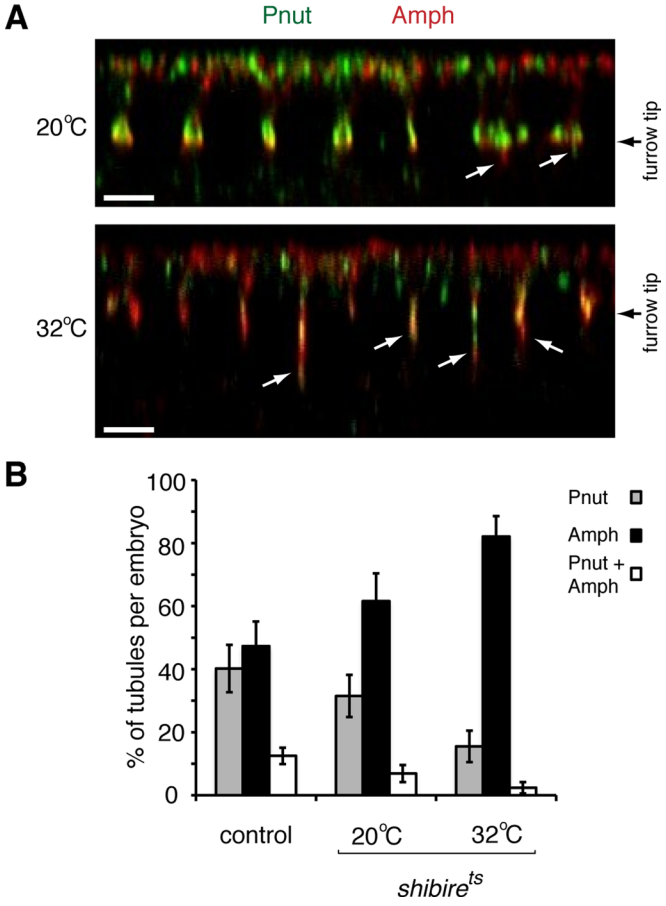

FIGURE 5: Dynamin activity is involved in establishing Pnut-positive CFT-tubules. (A) The *z*-sections of *shibire*^{ts} embryos at the permissive (20°C) and nonpermissive (32°C) temperatures stained with anti-Pnut and anti-amphiphysin (Amph) antibodies. White arrows point to CFT-tubules. Bar, 5 µm. (B) Quantification of the number of CFT-tubules staining positive for only Pnut, only amphiphysin (Amph), or both markers. Error bars, ± SD. Control, $n = 11$; *shibire*^{ts} 20°C, $n = 7$; and *shibire*^{ts} 32°C, $n = 8$.

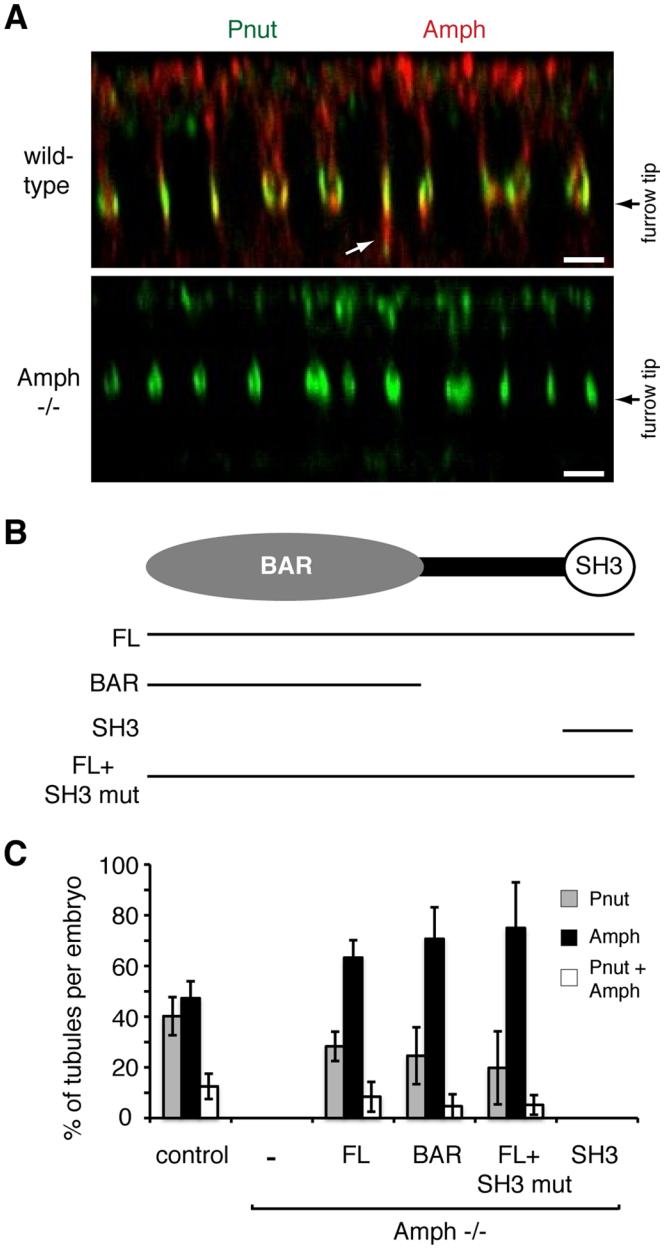

FIGURE 6: The BAR domain of amphiphysin is required for CFT-tubule formation. (A) The *z*-sections of control and amphiphysin-null *Drosophila* lines stained with anti-Pnut and anti-amphiphysin (Amph) antibodies. White arrow points to CFT-tubules. Bar, 5 µm. (B) Cartoon outlining the domain organization of amphiphysin and the different rescue construct expressed in amphiphysin-null *Drosophila*. (C) Quantitation of the number and type of CFT-tubules in different *Drosophila* lines. Error bars, ±SD. Localization in a minimum of 10 embryos for each condition was analyzed.

increased ($p < 0.0001$; Figure 5B). These data suggest that dynamin differentially influences CFT-tubule subpopulations.

Amphiphysin is required for Peanut-positive tubule formation

We next examined the role of amphiphysin in CFT-tubule formation. To determine whether amphiphysin was required for Peanut CFT-tubule formation, we analyzed CFT-tubules in a *Drosophila* amphiphysin-null mutant, *amph*^{5E3} (Leventis *et al.*, 2001). Cellularization is successfully completed in *amph*^{5E3} embryos, and the embryos develop in to adults (Leventis *et al.*, 2001). It is striking that in *amph*^{5E3} embryos, CFT-tubules could not be detected (Figure 6, A and C). Peanut localization remained at the tip of the ingressing furrow (Figure 6A), suggesting that CFT-tubule formation required amphiphysin. To determine whether the loss of CFT-tubules was indeed due to the absence of amphiphysin expression, we expressed full-length epitope-tagged amphiphysin (Figure 6B) in *amph*^{5E3} embryos that did not express endogenous amphiphysin. Expression of epitope-tagged, full-length amphiphysin rescued the formation of the different classes of CFT-tubules that were absent from *amph*^{5E3}-null embryos. The different classes of CFT-tubules included those decorated only by Peanut, those decorated only by amphiphysin, and those containing distinct Peanut and amphiphysin domains (Figure 6C). These data confirm that the failure to form CFT-tubules in *amph*^{5E3}-null embryos was due to the specific loss of amphiphysin function.

Amphiphysin is a multidomain protein containing a BAR domain and a SH3 domain, each of which can perform distinct functions (Figure 6B). The BAR domain interacts with membranes and promotes membrane curvature (Takei *et al.*, 1999). In contrast, the SH3

domain facilitates interactions with other proteins, including synaptojanin (David *et al.*, 1996), dynamin (Grabs *et al.*, 1997), and WASP (Zelhof *et al.*, 2001). To determine which domain of amphiphysin drives CFT-tubule formation, we expressed different epitope-tagged amphiphysin constructs (Figure 6B) in the *Drosophila amph*^{5E3}-null mutant and assessed CFT-tubule formation. When epitope-tagged amphiphysin-SH3 domain was expressed in *amph*^{5E3}-null mutant embryos, cleavage furrows formed; however, no amphiphysin antibody staining could be detected at the furrow tip, suggesting that the SH3 domain was not targeted to the cleavage furrow. Furthermore, no Peanut CFT-tubules or amphiphysin-positive CFT-tubules were observed in any of the embryos examined (Figure 6C). Because the failure of the SH3 domain to rescue CFT-tubule formation could be due to the failure of the epitope-tagged SH3 domain to be targeted to the cleavage furrow, we expressed a full-length amphiphysin cDNA that contained point mutations (G592R, P595L, and A596G) in the SH3 domain that disrupt SH3 domain function by prevent SH3 binding to target proline-rich regions (Zelhof *et al.*, 2001). The SH3-domain mutant amphiphysin was targeted to the tips of cleavage furrows and fully rescued the formation of all classes of CFT-tubules described earlier. Those classes of CFT-tubules include uniquely amphiphysin-positive and CFT-tubules and partially rescued the formation CFT-tubules that were uniquely Peanut positive and mixed-population CFT-tubules (Figure 6C). These data suggest that the SH3 has no significant role in stimulating CFT-tubule formation.

To determine whether the BAR domain was sufficient for CFT-tubule formation, we examined whether a construct containing an epitope-tagged amphiphysin BAR domain (Figure 6B) could rescue the defect in CFT-tubule formation observed in *amph*^{5E3}-null embryos. The epitope-tagged amphiphysin BAR domain was targeted to the tips of cleavage furrows and fully rescued the formation of CFT-tubules that were uniquely labeled with amphiphysin (Figure 6C) and partially rescued the formation of uniquely Peanut-positive and mixed-population CFT-tubules (Figure 6C). These data suggest that the BAR domain of amphiphysin is necessary and sufficient for the formation of all classes of CFT-tubules.

Amphiphysin and dynamin differentially regulate cleavage furrow ingression kinetics

Our data establish a role for both dynamin and amphiphysin in CFT-tubule formation and organization under conditions in which cleavage furrows still form and ingress. However, their disruption has opposite effects on CFT-tubules; disruption of dynamin causes the formation of elongated CFT-tubules, whereas disruption of amphiphysin inhibits CFT-tubule formation. Disruption of either protein does not affect cleavage formation, suggesting that CFT-tubules are not involved in cleavage furrow formation per se. However, it is possible that dynamin, amphiphysin, and CFT-tubules have roles in other aspects of cleavage furrow organization. To address this, we analyzed cleavage furrow ingression kinetics upon disruption of dynamin, when CFT-tubules are longer, and disruption of amphiphysin, when no CFT-tubules form.

Cleavage furrow ingression is a dynamic process that can be broken up into distinct phases: an initial phase that is very slow, then a slow phase, and then a fast phase (Field *et al.*, 2005a). To characterize the role of amphiphysin and dynamin in regulating cleavage furrow ingression kinetics, we observed ingression of the cleavage furrow during cellularization upon disruption of amphiphysin or dynamin by differential interference contrast (DIC) time-lapse microscopy as described by Field *et al.* (2005a). Our analysis confirmed three distinct phases of cleavage furrow ingression in wild-type embryos at room temperature (20°C): an initial phase with an ingression velocity of 0.08 ± 0.02 μm/min; a slow phase with an ingression velocity of 0.72 ± 0.17 μm/min, and a fast phase with an ingression velocity of 1.23 ± 0.33 μm/min (Figure 7A). Although the three distinct phases of cleavage furrow ingression were observed in

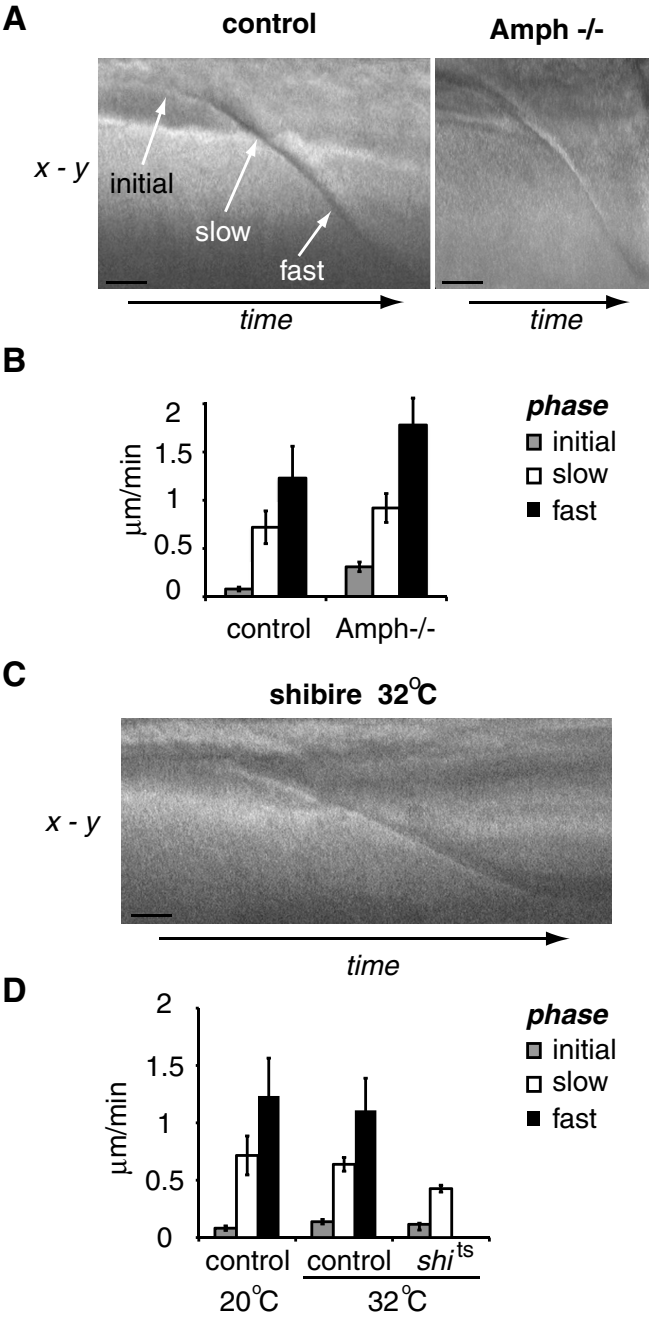

FIGURE 7: Amphiphysin and dynamin differentially regulate cleavage furrow ingression. (A) Representative kymographs of ingressing furrows in control and amphiphysin-null *Drosophila* lines. (B) Quantitation of the velocity of the different stages of furrow ingression during cellularization of embryos in A. Data were compiled from at least five embryos for each condition. (C) A representative kymograph of ingressing furrows in the *shibire*^{ts} *Drosophila* line at the nonpermissive temperature of 32°C. (D) Quantitation of the velocity of the different stages of furrow ingression during cellularization of embryos in C. Error bars, ±SD. Data were compiled from five embryos for each condition. Bar, 5 μm.

amph^{5E3}-mutant embryos, the kinetics of ingression differed from that of wild-type embryos. In embryos lacking amphiphysin, all phases of cleavage furrow ingression were faster (Figure 7B: initial, 0.31 ± 0.05 μm/min; slow, 0.93 ± 0.15 μm/min; and fast, 1.78 ± 0.28 μm/min). In particular, the final phase of furrow ingression was significantly faster in embryos lacking amphiphysin (1.78 ± 0.28 μm/min) compared with wild-type embryos (1.23 ± 0.33 μm/min; $p = 0.01$).

Next we examined the ability of dynamin to regulate the kinetics of furrow ingression (Figure 7, C and D). We found that cleavage furrow ingression was significantly slowed in *shibire*^{ts} embryos maintained at the nonpermissive temperature (32°C). Specifically, the rate of cleavage furrow ingression of the single slow phase was slower than the slow-phase cleavage furrow ingression of control embryo at the same temperature, 32°C (control, 0.64 ± 0.03 μm/min; *shibire*^{ts}, 0.43 ± 0.05 μm/min; $p < 0.01$). These data demonstrate a role for dynamin in the transition from the slow to the fast phase of cleavage furrow ingression.

DISCUSSION

Cellularization in the *Drosophila* embryo involves de novo generation of 6000 columnar epithelial cells, which are generated by the ingression of plasma membrane furrows—cleavage furrows—that enclose each nucleus (Mazumdar and Mazumdar, 2002). At the tip of ingressing cleavage furrows, CFT-tubules form. In this study, we demonstrate the existence of three populations of CFT-tubules, which can de defined by different septin family members. The different populations of CFT-tubules are differentially regulated, and their presence or absence correlates with changes in cleavage furrow ingression kinetics.

We identified septins as additional factors localizing to the CFT-tubules. Of interest, not all septins localize to the same CFT-tubules or the same domain within a single CFT-tubule. This suggests that although the CFT-tubules are formed by an endocytic pathway (Sokac and Wieschaus, 2008a), the tubules are not homogeneous. Instead, tubules can contain different domains that may have different functions. We identified three distinct types of tubules: those that contain only amphiphysin and the septins Sep1 and Sep2, those that contain only the septins Peanut, Sep4, and Sep5, and those that possess heterogeneous subdomains each defined by a distinct composition of these various components. Of importance, our localization studies suggest that distinct septin complexes localize to different structures. Because Peanut, Sep4, and Sep5 do not colocalize with Sep1 and Sep2 on CFT-tubules, we predict that Peanut, Sep4, and Sep5 form a novel septin complex. This new septin complex may resemble the previously isolated complex of Peanut, Sep1, and Sep2, as Sep2 is most closely related to Sep5 (72% identity) and Sep1 is most closely related to Sep4 (47% identity). We were not able to isolate individual septin complexes by immunoprecipitation, as all septins coimmunoprecipitated. This finding is consistent with studies in mammalian cells (Estey *et al.*, 2010) and reflects either the heterogeneous nature of septin complexes within the entire embryo or that we were, in part, immunoprecipitating partial septin filaments. Unexpectedly, Peanut did not colocalize with Sep1 and Sep2 on CFT-tubules. This observation raises the possibility that Sep1 and Sep2 alone form a complex. Septin filaments in yeast and mammalian systems are generated from octamers containing two copies of four different septins arranged in an inverted repeat (Kim *et al.*, 2011); however, this may not be true for all systems. In the case of *Drosophila* a hexamer of Peanut, Sep1, and Sep2 has been isolated (Field *et al.*, 1996), and in *Caenorhabditis elegans* there are only two septin genes (John *et al.*, 2007).

Septins have predominantly been implicated in modulating events at the plasma membrane in conjunction with the actin cytoskeleton (Adam *et al.*, 2000; Saarikangas and Barral, 2011; Spiliotis and Gladfelther, 2011; Mostowy and Cossart, 2012). In mammalian cells, septins have also been linked to potential roles in membrane trafficking, especially in the exocytic pathway, possibly by regulating vesicle fusion (Hsu *et al.*, 1998; Beites *et al.*, 1999, 2005; Vega and Hsu, 2003; Amin *et al.*, 2008). It seems unlikely that the septins on CFT-tubules are regulating exocytosis, as all evidence suggests that exocytosis occurs at distinct apical sites in the syncytial embryo (Pelissier *et al.*, 2003). In contrast, one study suggests a role for septins in the endocytic pathway by regulating recruitment of the coat protein complex AP-3 to lysosomal membranes (Baust *et al.*, 2008). The precise roles for septins in this process are unclear. In CFT-tubules, it is possible that septins exert an effect directly on the membrane. Septins can tubulate membranes containing phosphatidylinositol (4,5)-bisphosphate (Tanaka-Takiguchi *et al.*, 2009), a lipid that has a key role in cytokinesis (Field *et al.*, 2005b; Wong *et al.*, 2005). However, our data demonstrate that CFT-tubule formation is dependent on amphiphysin. Septins have been proposed to stabilize membranes (Gilden and Krummel, 2010). Therefore septins could stabilize the CFT-tubules once formed. Indeed, reduced recruitment of septins to cleavage furrows destabilizes the entire cleavage cleavage furrow (Field *et al.*, 2005a). Furthermore, embryos depleted of Peanut form unstable yolk channels at the end of cellularization (Adam *et al.*, 2000), further supporting the model that septins can stabilize membrane structures to which they localize. These findings also suggest that mutations that deplete septins will not allow examination of the role of septins in CFT-tubule organization and function.

We found that CFT-tubule formation requires the BAR domain of amphiphysin. The N-BAR subfamily, to which amphiphysin belongs, can bind to membranes and promote their curvature (reviewed in Masuda and Mochizuki, 2010; Suetsugu *et al.*, 2010). Amphiphysin is also involved in t-tubule formation in *Drosophila* indirect flight muscles (Razzaq *et al.*, 2001) and mouse heart muscle (Muller *et al.*, 2003). These findings suggest a conserved role for amphiphysin in promoting tubule formation and organization.

Loss of amphiphysin and the prevention of CFT-tubule formation did not inhibit furrow ingression, suggesting that amphiphysin is not required for remodeling of the membrane to drive furrow ingression. Instead, loss of amphiphysin increased the rate of furrow ingression. Because amphiphysin localizes to the tip of the furrow, it is possible that amphiphysin acts as a negative regulator of furrow ingression. Alternatively, by preventing CFT-tubule formation, amphiphysin may render more plasma membrane accessible for furrow ingression, and therefore the rate of furrow ingression increases. Consistent with this model, when CFT-tubules become longer upon disruption of dynamin, the rate of cleavage furrow ingression is reduced. One potential consequence of inhibiting endocytosis at the furrow tip would be to reduce the amount of membrane available for the expansion of the plasma membrane and the ingression of the furrow. In such a scenario membrane derived from endocytosis at the tip of the furrow would be recycled back to the plasma membrane through the exocytic pathway, thereby providing sufficient membrane for the expansion and ingression of the furrow. This reduced availability of membrane could manifest itself as a reduced rate of furrow ingression seen in *shibire*^{ts} embryos at the nonpermissive temperature, where CFT-tubules elongate due to a failure to pinch off. The additional membrane may be especially important for the rapid increase in furrow ingression we see once the furrow has ingressed ~10 μm, a depth

of ingression where CFT-tubules normally become shorter and disappear.

Changes in tubule parameters correlate with changes in cleavage furrow ingression kinetics, especially in the fast phase of ingression; longer, more persistent tubules correlate with slower ingression kinetics, and the absence of tubules correlates with faster ingression kinetics. If the fast phase of cleavage furrow ingression were dependent upon new membrane being inserted into the plasma membrane, then restricting membrane insertion would suppress the fast phase. If membrane was recycled by endocytosis at the cleavage furrow tips through an endocytic compartment back to the plasma membrane, then changes in CFT-tubule parameters might be expected to affect cleavage furrow ingression kinetics.

In the models outlined here CFT-tubules would function to buffer the amount of available membrane that is accessible for efficient cleavage furrow ingression. However, no comparable measurements have been made with respect to t-tubules in muscles. Therefore it remains unclear whether the tubules in these different systems have a common function, whether they are examples of specialized endocytosis, or whether the creation of extra membrane surface area facilitates specialized functions in these different systems.

MATERIALS AND METHODS

Fly stocks

The *D. melanogaster* lines used were w^{1118}, a Sep2-GFP line (Silverman-Gavrila *et al.*, 2008), the temperature-sensitive allele of dynamin (*shibire* allele shi^{1}; Poodry *et al.*, 1973), and an amphiphysin-null mutant line, $amph^{5E3}$, which was generated by imprecise P-element excision (Leventis *et al.*, 2001). The Sep1, Sep4, Sep5, and Peanut-GFP transgenes were constructed by using PCR to amplify the corresponding cDNA, and the product was cloned into the gateway TOPO cloning vector pCR8/GW/TOPO (Invitrogen, Carlsbad, CA). The cDNA was then recombined into the pUASP-adapted vector in frame with GFP (T. Murphy, Carnegie Institution of Washington, Washington, DC). Transgenic flies were then generated using standard methods (Rubin and Spradling, 1982). Expression of pUASP constructs was induced using P[GAL4::VP16-nos.UTR] (Van Doren *et al.*, 1998).

Different deletion constructs of *amph* were generated using PCR with template DNA from the expressed sequence tag LD19810, containing the full-length amphiphysin cDNA (amino acids 1–602), as follows. A PCR product of the full-length amphiphysin cDNA was subcloned into the pUAST vector containing a C-terminal V5 tag. For the remaining constructs, PCR products were cloned the into the pENTER vector (Invitrogen). For the Amph-BAR domain a fragment encoding amino acids 1–245 was amplified, and for the Amph-SH3 domain a fragment encoding amino acids 523–602. For the Amph-SH3 mutant construct, the same mutations (G592R, P595L, and A596G) were made as previously described (Zelhof *et al.*, 2001) using the QuikChange Mutagenesis Kit (Stratagene, Santa Clara, CA). Subsequently amphiphysin fragments and mutations were recombined into the pTWM DESTINATION Gateway vector (a modified pDESTINATION vector with a UAS promoter sequence and a C-terminal 6×-myc tag, as modified by the Murphy lab [http://emb.carnegiescience.edu/labs/murphy/Gateway%20vectors.html]). The tagged constructs were subsequently injected into w-flies (BestGene, Chino Hills, CA) and double balanced using the w1118; Sp/CyO-GFP; Sb/TM3Ser line.

Embryo fixation and immunofluorescence

The 0- to 3-h embryos were collected, washed in water, and dechorionated by incubating in 50% (vol/vol) bleach for 1 min. Embryos were rinsed in water and then added to vials containing heptane. For methanol fixation, an equal volume of methanol was added and the embryos vigorously agitated for 1 min. Devitellated embryos were removed and washed a further three times in methanol. Embryos were then either stored in methanol at –20°C or stained immediately. For formaldehyde fixation an equal volume of 3.7% formaldehyde, 10 mM 1,4-piperazinediethanesulfonic acid, pH 6.9, 0.2 mM ethylene glycol tetraacetic acid, and 0.1 mM $MgSO_4$ was added to embryos in heptane, which were then vigorously agitated for 20 min. The aqueous phase was then removed and replaced with an equal volume of methanol, and embryos were further processed as described.

To immunostain embryos, they were first rehydrated by two 5-min incubations in PBST (PBS containing 0.5% bovine serum albumin and 0.1% Triton X-100). Embryos were further blocked in PBST for 60 min. Embryos were incubated in primary antibody diluted in PBST for 60 min with gentle agitation and then washed by four 5-min incubations in PBST. Next embryos were incubated in secondary antibodies conjugated with Alexa 488, Alexa 594 or Alexa 647 (Invitrogen) diluted 1:1000 in PBST. After washing as described, embryos were cleared in mounting media (90% glycerol, 20 mM Tris, pH 8.8, 0.5% *p*-phenylenediamine) overnight, then mounted in the same media. Images of stained embryos were captured with a Plan Apochromat 60× 1.5/numerical aperture (NA) 1.0 oil immersion lens mounted on a Nikon Eclipse TE2000-E inverted microscope (Nikon, Melville, NY) equipped with a spinning disk confocal (PerkinElmer, Waltham, MA) equipped with an Orca-EM charge-coupled device camera (Hamamatsu, Hamamatsu, Japan) driven by MetaMorph software (Universal Imaging, Downingtown, PA).

Antibodies used in the study include anti-peanut (Neufeld and Rubin, 1994; Developmental Studies Hybridoma Bank, Iowa City, IA), anti-anillin (Goldbach *et al.*, 2010), and anti-amphiphysin (Leventis *et al.*, 2001).

Embryo extract and immunoprecipitation

The 0- to 3-h embryo extract was prepared as previously described (Nelson *et al.*, 2004). Immunoprecipitations were performed and analyzed as previously described (Silverman-Gavrila *et al.*, 2008), using the anti-Peanut antibody or an anti-GFP antibody (Roche, Indianapolis, IN).

DIC microscopy

The 0- to 2-h embryos were collected and dechorionated as described. Embryos were mounted between two 25-mm-diameter coverslips on double-sided sticky tape (Scotch; 3M, St. Paul, MN) under halocarbon oil (Halocarbon Products, River Edge, NJ). The mounted embryos were placed on a temperature-controlled stage (Harvard Apparatus, Holliston, MA) mounted on a Nikon E-800 microscope and visualized using a Plan Apochromat 40× 1.5/NA 1.0 oil immersion lens using an Orca ER camera (Hamamatsu). Images were taken every 10 s. Rates of ingression were calculated using the slopes from kymographs generated using MetaMorph.

ACKNOWLEDGMENTS

We thank B. Lavoie and J. Brill for reading the manuscript. G.B. is supported by a grant from the Natural Sciences and Engineering Council of Canada and a Tier I Canada Research Chair in Molecular and Developmental Neurobiology. A.W. is supported by grants from the Canadian Cancer Society and the Natural Sciences and Engineering Council of Canada, and B.C. was supported by a Restracomp Award from The Hospital for Sick Children.

REFERENCES

Adam JC, Pringle JR, Peifer M (2000). Evidence for functional differentiation among *Drosophila* septins in cytokinesis and cellularization. Mol Biol Cell 11, 3123–3135.

Amin ND, Zheng YL, Kesavapany S, Kanungo J, Guszczynski T, Sihag RK, Rudrabhatla P, Albers W, Grant P, Pant HC (2008). Cyclin-dependent kinase 5 phosphorylation of human septin SEPT5 (hCDCrel-1) modulates exocytosis. J Neurosci 28, 3631–3643.

Baust T, Anitei M, Czupalla C, Parshyna I, Bourel L, Thiele C, Krause E, Hoflack B (2008). Protein networks supporting AP-3 function in targeting lysosomal membrane proteins. Mol Biol Cell 19, 1942–1951.

Beites CL, Campbell KA, Trimble WS (2005). The septin Sept5/CDCrel-1 competes with alpha-SNAP for binding to the SNARE complex. Biochem J 385, 347–353.

Beites CL, Xie H, Bowser R, Trimble WS (1999). The septin CDCrel-1 binds syntaxin and inhibits exocytosis. Nat Neurosci 2, 434–439.

David C, McPherson PS, Mundigl O, de Camilli P (1996). A role of amphiphysin in synaptic vesicle endocytosis suggested by its binding to dynamin in nerve terminals. Proc Natl Acad Sci USA 93, 331–335.

Estey MP, Di Ciano-Oliveira C, Froese CD, Bejide MT, Trimble WS (2010). Distinct roles of septins in cytokinesis: SEPT9 mediates midbody abscission. J Cell Biol 191, 741–749.

Field CM, al-Awar O, Rosenblatt J, Wong ML, Alberts B, Mitchison TJ (1996). A purified *Drosophila* septin complex forms filaments and exhibits GTPase activity. J Cell Biol 133, 605–616.

Field CM, Coughlin M, Doberstein S, Marty T, Sullivan W (2005a). Characterization of anillin mutants reveals essential roles in septin localization and plasma membrane integrity. Development 132, 2849–2860.

Field S, Madson N, Kerr M, Galbraith K, Kennedy C, Tahiliani M, Wilkins A, Cantley L (2005b). PtdIns(4,5)P2 functions at the cleavage furrow during cytokinesis. Curr Biol 15, 1407–1412.

Gilden J, Krummel MF (2010). Control of cortical rigidity by the cytoskeleton: emerging roles for septins. Cytoskeleton 67, 477–486.

Goldbach P, Wong R, Beise N, Sarpal R, Trimble WS, Brill JA (2010). Stabilization of the actomyosin ring enables spermatocyte cytokinesis in *Drosophila*. Mol Biol Cell 21, 1482–1493.

Grabs D, Slepnev VI, Songyang Z, David C, Lynch M, Cantley LC, De Camilli P (1997). The SH3 domain of amphiphysin binds the proline-rich domain of dynamin at a single site that defines a new SH3 binding consensus sequence. J Biol Chem 272, 13419–13425.

Graveley BR *et al*. (2011). The developmental transcriptome of *Drosophila melanogaster*. Nature 471, 473–479.

Hsu SC, Hazuka CD, Roth R, Foletti DL, Heuser J, Scheller RH (1998). Subunit composition, protein interactions, and structures of the mammalian brain sec6/8 complex and septin filaments. Neuron 20, 1111–1122.

Hurly JH, Boura E, Carlson LA, Rozycki B (2010). Membrane budding. Cell 142, 875–887.

John CM *et al*. (2007). The *Caenorhabditis elegans* septin complex is nonpolar. EMBO J 26, 3296–3307.

Kaksonen M, Sun Y, Drubin DG (2003). A pathway for association of receptors, adaptors, and actin during endocytic internalization. Cell 115, 475–487.

Kaksonen M, Toret CP, Drubin DG (2005). A modular design for the clathrin- and actin-mediated endocytosis machinery. Cell 123, 305–320.

Kim MS, Froese CD, Estey MP, Trimble WS (2011). SEPT9 occupies the terminal positions in septin octamers and mediates polymerization-dependent functions in abscission. J Cell Biol 195, 815–826.

Kochubey O, Majumdar A, Klingauf J (2006). Imaging clathrin dynamics in *Drosophila melanogaster* hemocytes reveals a role for actin in vesicle fission. Traffic 7, 1614–1627.

Levayer R, Lecuit T (2012). Biomechanical regulation of contractility: spatial control and dynamics. Trends Cell Biol 22, 61–81.

Leventis P, Chow B, Stewart B, Iyengar B, Campos A, Boulianne G (2001). *Drosophila* amphiphysin is a post- synaptic protein required for normal locomotion but not endocytosis. Traffic 2, 839–850.

Liu J, Fairn GD, Ceccarelli DF, Sicheri F, Wilde A (2012). Cleavage furrow organization requires PIP2-mediated recruitment of anillin. Curr Biol 22, 64–69.

Masuda M, Mochizuki N (2010). Structural characteristics of BAR domain superfamily to sculpt the membrane. Semin Cell Dev Biol 21, 391–398.

Mazumdar A, Mazumdar M (2002). How one becomes many: blastoderm cellularization in *Drosophila melanogaster*. BioEssays 24, 1012–1022.

Merrifield CJ, Feldman ME, Wan L, Almers W (2002). Imaging actin and dynamin recruitment during invagination of single clathrin-coated pits. Nat Cell Biol 4, 691–698.

Mostowy S, Cossart P (2012). Septins: the fourth component of the cytoskeleton. Nat Rev Mol Cell Biol 13, 183–194.

Muller AJ *et al*. (2003). Targeted disruption of the murine Bin1/Amphiphysin II gene does not disable endocytosis but results in embryonic cardiomyopathy with aberrant myofibril formation. Mol Cell Biol 23, 4295–4306.

Nelson MR, Leidal AM, Smibert CA (2004). *Drosophila* Cup is an eIF4E-binding protein that functions in Smaug-mediated translational repression. EMBO J 23, 150–159.

Neufeld TP, Rubin GM (1994). The *Drosophila* peanut gene is required for cytokinesis and encodes a protein similar to yeast putative bud neck filament proteins. Cell 77, 371–379.

Pelissier A, Chauvin JP, Lecuit T (2003). Trafficking through Rab11 endosomes is required for cellularization during *Drosophila* embryogenesis. Curr Biol 13, 1848–1857.

Poodry CA, Hall L, Suzuki DT (1973). Developmental properties of Shibire: a pleiotropic mutation affecting larval and adult locomotion and development. Dev Biol 32, 373–386.

Razzaq A, Robinson IM, McMahon HT, Skepper JN, Su Y, Zelhof AC, Jackson AP, Gay NJ, O'Kane CJ (2001). Amphiphysin is necessary for organization of the excitation-contraction coupling machinery of muscles, but not for synaptic vesicle endocytosis in *Drosophila*. Genes Dev 15, 2967–2979.

Ridley AJ ((2011). Life at the leading edge. Cell 145, 1012–1022.

Riggs B, Fasulo B, Royou A, Mische S, Cao J, Hays TS, Sullivan W (2007). The concentration of Nuf, a Rab11 effector, at the microtubule-organizing center is cell cycle regulated, dynein-dependent, and coincides with furrow formation. Mol Biol Cell 18, 3313–3322.

Rorth P (1998). Gal4 in the *Drosophila* female germline. Mech Dev 78, 113–118.

Rubin GM, Spradling AC (1982). Genetic transformation of *Drosophila* with transposable element vectors. Science 218, 348–353.

Saarikangas J, Barral Y (2011). The emerging functions of septins in metazoans. EMBO Rep 12, 1118–1126.

Schmid SL, Frolov VA (2011). Dynamin: functional design of a membrane fission catalyst. Annu Rev Cell Dev Biol 27, 79–105.

Silverman-Gavrila R, Hales K, Wilde A (2008). Anillin-mediated targeting of Peanut to pseudocleavage furrows is regulated by the GTPase Ran. Mol Biol Cell 19, 3735–3744.

Sokac AM, Wieschaus E (2008a). Local actin-dependent endocytosis is zygotically controlled to initiate *Drosophila* cellularization. Dev Cell 14, 775–786.

Sokac AM, Wieschaus E (2008b). Zygotically controlled F-actin establishes cortical compartments to stabilize furrows during *Drosophila* cellularization. J Cell Sci 121, 1815–1824.

Spiliotis ET, Gladfelther AS (2011). Spatial guidance of cell asymmetry: septin GTPases show the way. Traffic 13, 195–203.

Spiliotis ET, Kinoshita M, Nelson WJ (2005). A mitotic septin scaffold required for mammalian chromosome congression and segregation. Science 307, 1781–1785.

Suetsugu S, Toyooka K, Senju Y (2010). Subcellular membrane curvature mediated by the BAR domain superfamily proteins. Semin Cell Dev Biol 21, 340–349.

Sun Y, Martin AC, Drubin DG (2006). Endocytic internalization in budding yeast requires coordinated actin nucleation and myosin motor activity. Dev Cell 11, 33–46.

Takei K, Slepnev VI, Haucke V, De Camilli P (1999). Functional partnership between amphiphysin and dynamin in clathrin-mediated endocytosis. Nat Cell Biol 1, 33–39.

Tanaka-Takiguchi Y, Kinoshita M, Takiguchi K (2009). Septin-mediated uniform bracing of phospholipid membranes. Curr Biol 19, 140–145.

Van Doren M, Williamson AL, Lehmann R (1998). Regulation of zygotic gene expression in *Drosophila* primordial germ cells. Curr Biol 8, 243–246.

Vega IE, Hsu SC (2003). The septin protein Nedd5 associates with both the exocyst complex and microtubules and disruption of its GTPase activity promotes aberrant neurite sprouting in PC12 cells. Neuroreport 14, 31–37.

Wong R, Hadjiyanni I, Wei HC, Polevoy G, McBride R, Sem KP, Brill JA (2005). PIP2 hydrolysis and calcium release are required for cytokinesis in *Drosophila* spermatocytes. Curr Biol 15, 1401–1406.

Yarar D, Waterman-Storer CM, Schmid SL (2005). A dynamic actin cytoskeleton functions at multiple stages of clathrin-mediated endocytosis. Mol Biol Cell 16, 964–975.

Zelhof AC, Bao H, Hardy RW, Razzaq A, Zhang B, Doe CQ (2001). *Drosophila* amphiphysin is implicated in protein localization and membrane morphogenesis but not in synaptic vesicle endocytosis. Development 128, 5005–5015.